

ACKNOWLEDGMENT

The work described in this paper was carried out with the help of the Centre National de la Recherche Scientifique. The authors are indebted to Prof. Barriol for several helpful discussions, his continued interest, and encouragement.

REFERENCES

- [1] A. F. Harvey, *Microwave Engineering*. New York: Académie 1963.
- [2] F. Horner, T. A. Taylor, R. Dunsmuir, J. Lamb, and W. Jackson, "Resonance methods of dielectric measurement at centimeter wavelengths," *J. Instn Elect. Engrs (GB)*, vol. 93, pt. III, pp. 53-68, 1946. J. Lamb, "Dielectric measurement at wavelengths around 1 cm by means of an H_{01} cylindrical cavity resonator," *J. Instn Elect. Engrs (GB)*, vol. 93, pt. IIIA, p. 1447, 1946.
- [3] A. Von Hippel, *Dielectric Materials and Applications*. New York: Wiley, 1954.
- [4] Howard E. Bussey, "Cavity resonator dielectric measurements on rod samples," *1959 Ann. Rept. Conf. on Electrical Insulation*, Nat'l Acad. of Sciences NRC, No. 756, January 1960. Also reprinted in *Insulation*, November 1960.
- [5] C. H. Collie, J. B. Hasted, and D. M. Ritson, "The cavity resonator method of measuring the dielectric constants of polar liquids in the centimeter band," *Proc. Phys. Soc.*, vol. 60, pp. 71-82, 1948.
- [6] R. P. Penrose, "Some measurements of the permittivity and power factor of low loss solids at 25.000 Mcs frequency," *Trans. Faraday Soc. (GB)*, vol. 42A, pp. 108-114, 1946.
- [7] G. Roussy and M. Felden, "Analyse matricielle d'une cavité résonnante en U.H.F.," *J. Physique appliquée*, vol. 26, p. 11 A, January, 1965.
- [8] G. Roussy, "Mesures à fréquence fixe de la constante diélectrique complexe des solides à l'aide d'une cavité résonnante," *J. Physique appliquée*, vol. 26, p. 64 A, February 1965.

The Cutoff Wavelength of the TE_{10} Mode in Ridged Rectangular Waveguide of Any Aspect Ratio

J. R. PYLE

Abstract—Design curves for ridged rectangular waveguides of the usual aspect ratio of 0.45 were published by Hopfer following earlier work carried out by Cohn and Marcuvitz.

This paper has been written to extend the design data to ridged rectangular waveguides of any aspect ratio. An analysis of the error introduced by proximity effects has shown these to be of the order of a few percent.

I. INTRODUCTION

PUBLISHED design information on ridged rectangular waveguides may be found in the *Waveguide Handbook* [1] and in papers by Cohn [2] and Hopfer [3]. Hopfer gives design curves for the cutoff wavelength λ_c of the TE_{10} mode in single and double-ridged rectangular waveguide of the usual aspect ratio of 0.45. For other aspect ratios he provides correction curves, which, he states, are essentially a first-order correction on the value of the cutoff wavelength at the aspect ratio of 0.45.

The purpose of this paper is:

- 1) to repeat Hopfer's work for the single and double ridge in rectangular waveguide of an aspect ratio of 0.45, and to present the design data in tabulated form to permit accurate interpolation between computed values;
- 2) to extend the design data to cover aspect ratios

other than 0.45 while maintaining the same accuracy as for the above case, and to present this information graphically as a correction to be applied to the values for an aspect ratio of 0.45; and

- 3) to investigate the errors which are introduced by such proximity effects as narrow ridges and well-formed ridges near the side wall of the waveguide.

II. CUTOFF CONDITION OF THE TE_{10} MODE IN RECTANGULAR WAVEGUIDE

Consider the rectangular waveguide shown in Fig. 1 where a and b are the transverse dimensions and b/a is the aspect ratio. The transmission of the TE_{10} wave within the metal walls may be represented by two converging TEM waves of free space wavelength λ_0 and angle 2θ between wave fronts. From the geometry of the system it follows that

$$\cos \theta = \frac{\lambda_0}{2a}. \quad (1)$$

The TE_{10} wave is cut off when θ is zero and when the TEM wave is traveling normally to the axis of the waveguide. This condition occurs at the cutoff wavelength λ_c given by

$$\lambda_c = 2a. \quad (2)$$

The cutoff wavelength could have been obtained in another way, by considering the rectangular waveguide

Manuscript received February 19, 1965; revised August 30, 1965.
The author is with the Weapons Research Establishment, Department of Supply, Salisbury, South Australia.

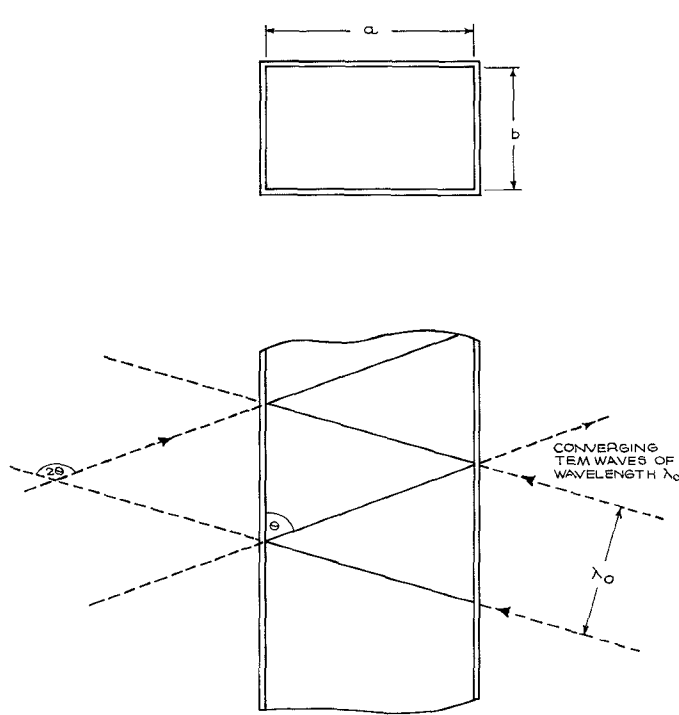


Fig. 1. TE wave between metal walls represented by converging TEM waves.

in Fig. 2 under the cutoff conditions of the TE_{10} mode. Since the TEM wave travels across the cross section, the latter may be represented by the equivalent circuit shown, where Z is the characteristic impedance of the parallel plate line of height b , and ϕ is the electrical length corresponding to $a/2$. The parallel plate line is terminated in a short circuit representing the waveguide wall.

The input voltage and current of the equivalent circuit may be represented by the matrix equation

$$\begin{bmatrix} V_{IN} \\ I_{IN} \end{bmatrix} = \begin{bmatrix} \cos \phi & jZ \sin \phi \\ j \sin \phi & \frac{1}{Z} \cos \phi \end{bmatrix} \begin{bmatrix} 0 \\ 1 \end{bmatrix}. \quad (3)$$

The input impedance Z_{IN} is

$$\begin{bmatrix} V_{IN} \\ I_{IN} \end{bmatrix} = Z \tan \phi.$$

At cutoff conditions Z_{IN} is infinite, a condition which is satisfied by

$$\phi = \frac{\pi}{2}$$

and since

$$\phi = \frac{\pi a}{\lambda_c}$$

by

$$\lambda_c = 2a.$$

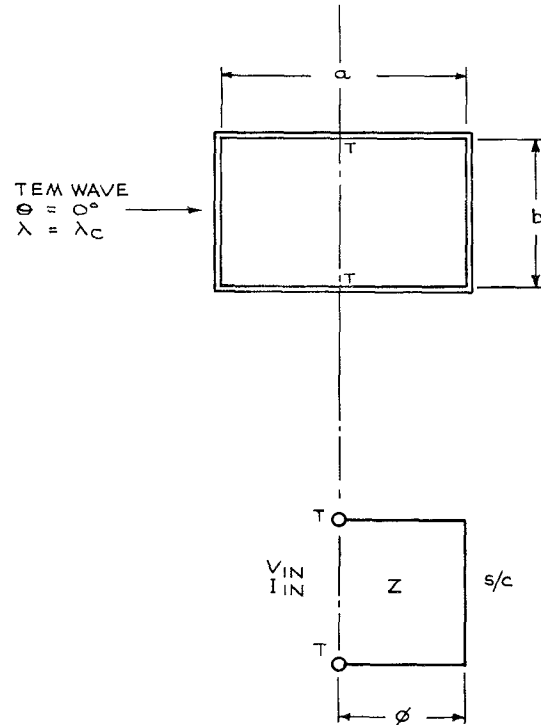


Fig. 2. Equivalent transverse circuit of rectangular waveguide at cutoff condition of the TE_{10} mode.

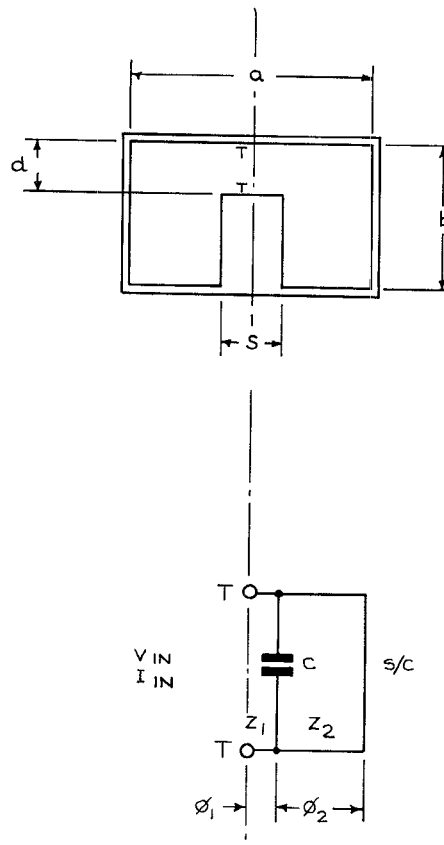
The second method used to obtain λ_c for the rectangular waveguide will be used in the case of a rectangular waveguide with a single or double rectangular ridge.

III. CUTOFF CONDITION OF THE TE_{10} MODE IN RIDGED RECTANGULAR WAVEGUIDE

Consider first the rectangular waveguide with a single rectangular ridge of width s and height $(b-d)$ as shown in Fig. 3. At the cutoff condition of the TE_{10} wave we may represent the cross section by the equivalent circuit shown where:

- 1) C is a discontinuity capacity dependent on the height of the ridge and represents the effect of modes of higher order than the fundamental TEM mode. The higher order modes have been introduced by the presence of the ridge and together with the fundamental TEM mode give the field configuration for ridged rectangular waveguide.
- 2) Z_1 and Z_2 are the characteristic impedances of the parallel plate lines of heights $(b-d)$ and b , respectively.
- 3) ϕ_1 and ϕ_2 are the electrical lengths associated with these lines.

The rectangular waveguide with a double rectangular ridge, each of width s , is shown in Fig. 4 where d is the spacing between the ridges. This symmetrical system may be analyzed in the same way as the single ridge by considering one of the half sections formed by introducing a conducting plane, as shown. The aspect ratio of the half section is $b/2a$, but the effect of the discon-



EQUIVALENT CIRCUIT AT TT

Fig. 3. Equivalent transverse circuit of rectangular waveguide with a single rectangular ridge at cutoff condition of the TE₁₀ mode.

tinuity capacity C , which is a function of b/d , is unchanged.

To determine the cutoff wavelength λ_c of a single or double-ridged rectangular waveguide using the equivalent circuit given in Fig. 3 or Fig. 4 we proceed as follows.

The input voltage V_{IN} and input current I_{IN} at terminals TT is given by the matrix equation:

$$\begin{bmatrix} V_{IN} \\ I_{IN} \end{bmatrix} = \begin{bmatrix} \cos \phi_1 & jZ_1 \sin \phi_1 \\ j \sin \phi_1 & \cos \phi_1 \end{bmatrix} \begin{bmatrix} 1 & 0 \\ jB & 1 \end{bmatrix} \cdot \begin{bmatrix} \cos \phi_2 & jZ_2 \sin \phi_2 \\ j \sin \phi_2 & \cos \phi_2 \end{bmatrix} \begin{bmatrix} 0 \\ 1 \end{bmatrix} \quad (4)$$

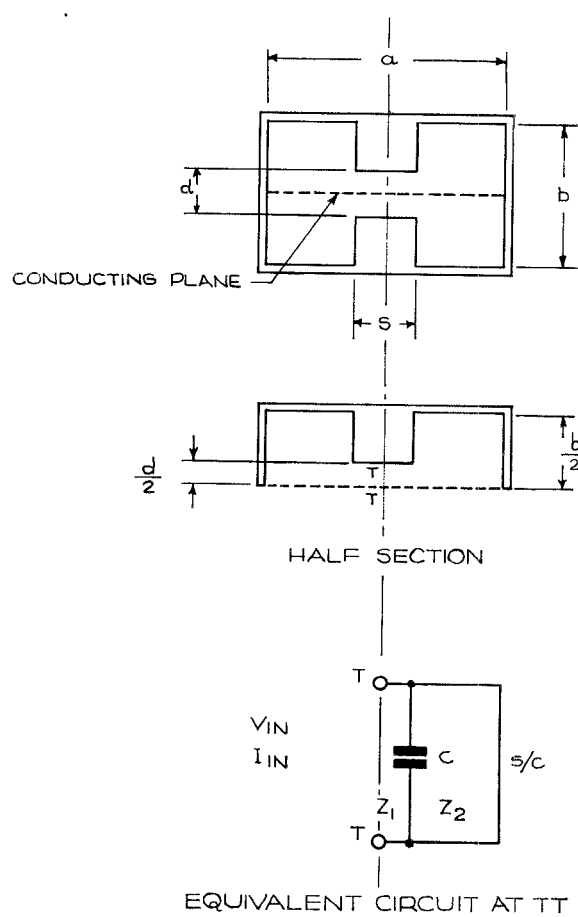
where

$$B = \frac{2\pi v C}{\lambda_c} \quad (5)$$

and

v = the velocity of propagation of an EM wave in the medium of the guide.

The cutoff condition occurs when Z_{IN} or V_{IN}/I_{IN} is

Fig. 4. Equivalent transverse circuit of rectangular waveguide with a double rectangular ridge at cutoff condition of the TE₁₀ mode.

infinite, or when

$$1 - \frac{Z_2}{Z_1} \tan \phi_1 \tan \phi_2 - B Z_2 \tan \phi_2 = 0. \quad (6)$$

The above equation is a transcendental equation in λ_c . It may be solved for λ_c by suitably programming a high speed digital computer. The normalized discontinuity susceptance BZ_2 plays an important role in the calculation of λ_c and will be discussed next.

IV. THE NORMALIZED DISCONTINUITY SUSCEPTANCE

The normalized discontinuity susceptance BZ_2 for a step ratio $\alpha = d/b$ between parallel plate lines has been obtained by Marcuvitz [4] and is accurate to one percent in the range $b < \lambda_c$.

Marcuvitz's expression contains two terms:

- 1) a dc term $[T_1(\lambda_c/4b)]$ which is predominant and is given by

$$T_1 \frac{\lambda_c}{4b} = \ln \left[\frac{1 - \alpha^2}{4\alpha} \right] \left[\frac{1 + \alpha}{1 - \alpha} \right]^{1/2}$$

$$\cdot \left[\alpha + \frac{1}{\alpha} \right], \quad \text{and} \quad (7)$$

- 2) a frequency dependent term $[T_2(\lambda_c/4b)]$ which is given by

$$T_2 \frac{\lambda_c}{4b} = \frac{4b}{\lambda_c} \left[2 \left[\frac{A + A^1 + 2C}{AA^1 - C^2} \right] + \left[\frac{2b}{4\lambda_c} \right]^2 \left[\frac{1-\alpha}{1+\alpha} \right]^{4\alpha} \left[\frac{5\alpha^2 - 1}{1 - \alpha^2} + \frac{4\alpha^2 C}{3A} \right]^2 \right] \quad (8)$$

where

$$A = \left[\frac{1+\alpha}{1-\alpha} \right]^{2\alpha} \left[\frac{1 + \sqrt{(1 - (2b/\lambda_c)^2)}}{1 - \sqrt{(1 - (2b/\lambda_c)^2)}} \right] - \frac{1 + 3\alpha^2}{1 - \alpha^2}$$

$$A^1 = \left[\frac{1+\alpha}{1-\alpha} \right]^{2\alpha} \left[\frac{1 + \sqrt{(1 - (2d/\lambda_c)^2)}}{1 - \sqrt{(1 - (2d/\lambda_c)^2)}} \right] + \frac{3 + \alpha^2}{1 - \alpha^2}$$

$$C = \left[\frac{4\alpha}{1 - \alpha^2} \right]^2.$$

The normalized discontinuity susceptance for a step ratio $\alpha = d/b$ between two infinite parallel plate lines of heights d and b is given by

$$BZ_2 = T_1 + T_2. \quad (9)$$

In the analysis of ridged waveguides at cutoff it is not possible to have two infinite parallel plate lines on either

side of the step. When the ridge is very narrow the interaction between the fringing field discontinuities across the top of the ridge must be considered. When the ridge is very close to the side wall of the waveguide, then the proximity effect of the metal plate must be considered.

A detailed account of these proximity effects and the errors introduced by them is given in the Appendix. For the purposes of computing design data it is sufficient to say that (9) may be rewritten for the case of ridged waveguides as

$$BZ_2 = P(T_1 + T_2) \quad (10)$$

where

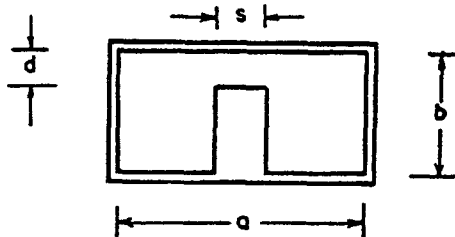
$$P = \coth \left[\frac{\pi(a - s)}{2b} \right].$$

The error in computing λ_c/a using (10) is shown in the Appendix to be

- one to three percent for the worst case of a diaphragm ridge ($s/a \ll 1$),
- three percent for the worst case $s/a = 0.9$, $d/b = 1/9$ for the waveguide of $b/a = 0.45$ when the above expression for P is used.

TABLE I
COMPUTED VALUES OF λ_c/a FOR $b/a = 0.45$ —SINGLE RIDGE

s/a	d/b	0.05	0.10	0.15	0.20	0.25	0.30	0.35	0.40	0.45	0.50	0.55	0.60	0.65	0.70	0.75	0.80	0.85	0.90	0.95
0.05	5.156	4.271	3.817	3.508	3.273	3.080	2.918	2.777	2.653	2.543	2.445	2.358	2.281	2.214	2.155	2.106	2.066	2.034	2.012	
0.10	5.823	4.643	4.072	3.701	3.425	3.206	3.023	2.866	2.730	2.609	2.502	2.407	2.322	2.248	2.183	2.128	2.081	2.044	2.017	
0.15	6.348	4.942	4.280	3.859	3.551	3.309	3.110	2.940	2.794	2.665	2.550	2.448	2.358	2.278	2.208	2.147	2.096	2.054	2.022	
0.20	6.764	5.181	4.447	3.985	3.652	3.392	3.179	3.000	2.845	2.709	2.589	2.482	2.387	2.303	2.228	2.163	2.108	2.062	2.026	
0.25	7.090	5.368	4.577	4.083	3.729	3.455	3.232	3.045	2.884	2.743	2.619	2.508	2.410	2.322	2.245	2.177	2.118	2.069	2.030	
0.30	7.338	5.509	4.672	4.154	3.785	3.500	3.270	3.077	2.911	2.767	2.640	2.527	2.426	2.337	2.257	2.187	2.126	2.075	2.033	
0.35	7.515	5.605	4.736	4.199	3.819	3.527	3.292	3.095	2.927	2.781	2.652	2.538	2.436	2.346	2.265	2.194	2.132	2.079	2.035	
0.40	7.627	5.661	4.769	4.221	3.833	3.537	3.299	3.100	2.931	2.785	2.656	2.541	2.440	2.349	2.269	2.198	2.135	2.082	2.036	
0.45	7.676	5.677	4.773	4.218	3.827	3.530	3.291	3.093	2.924	2.778	2.650	2.537	2.437	2.347	2.268	2.198	2.136	2.082	2.037	
0.50	7.665	5.655	4.747	4.191	3.801	3.505	3.268	3.072	2.906	2.762	2.636	2.526	2.428	2.340	2.263	2.194	2.134	2.082	2.037	
0.55	7.593	5.593	4.691	4.141	3.755	3.463	3.231	3.038	2.876	2.736	2.614	2.507	2.412	2.328	2.253	2.188	2.130	2.079	2.036	
0.60	7.460	5.491	4.605	4.066	3.689	3.404	3.178	2.991	2.834	2.700	2.583	2.480	2.390	2.310	2.240	2.177	2.123	2.075	2.035	
0.65	7.250	5.346	4.487	3.965	3.601	3.327	3.109	2.931	2.781	2.653	2.543	2.446	2.362	2.287	2.222	2.164	2.114	2.070	2.032	
0.70	6.991	5.157	4.335	3.836	3.490	3.230	3.024	2.856	2.716	2.596	2.494	2.405	2.327	2.259	2.200	2.148	2.103	2.063	2.029	
0.75	6.643	4.917	4.145	3.678	3.354	3.111	2.921	2.766	2.637	2.529	2.436	2.356	2.287	2.226	2.174	2.129	2.089	2.055	2.025	
0.80	6.204	4.619	3.912	3.485	3.190	2.970	2.798	2.660	2.545	2.449	2.358	2.299	2.240	2.189	2.145	2.107	2.074	2.046	2.021	
0.85	5.652	4.250	3.626	3.250	2.992	2.801	2.653	2.534	2.438	2.358	2.291	2.235	2.186	2.147	2.112	2.083	2.057	2.035	2.016	
0.90	4.946	3.786	3.270	2.961	2.751	2.597	2.480	2.387	2.314	2.254	2.205	2.164	2.130	2.101	2.077	2.057	2.039	2.024	2.011	
0.95	3.995	3.173	2.807	2.590	2.447	2.345	2.270	2.213	2.169	2.135	2.107	2.085	2.067	2.052	2.040	2.029	2.020	2.012	2.006	



V. THE CALCULATION OF λ_c

To solve the transcendental equation (6) in λ_c by an iterative method for a complete range of values for s and d at constant b/a ratio, we proceed as follows:

1) solve (6) on setting

$$BZ_2 = PT_1, \text{ and}$$

2) obtain an accurate solution, using the λ_c value obtained in (1) to solve (6) when

$$BZ_2 = P(T_1 + T_2).$$

Values of λ_c have been computed on an IBM 7090 machine for

$\frac{b}{a}$ values in the range 0.1 (0.1) 1.0

$\frac{s}{a}$ values in the range 0.05 (0.05) 0.95

$\frac{d}{b}$ values in the range 0.05 (0.05) 0.95

for the case of a single rectangular ridge in rectangular waveguide.

The values of λ_c for the double-ridged rectangular waveguide may be obtained from the value for the half section.

VI. THE COMPUTED RESULTS

Computed values of λ_c/a for a single rectangular ridge in a rectangular waveguide of b/a ratio equal to 0.45 are shown in Table I.

Computed values of λ_c/a for a double rectangular ridge in a rectangular waveguide of b/a ratio equal to 0.45 are shown in Table II.

The computed value of λ_c/a for a single rectangular ridge in a rectangular waveguide of any aspect ratio may be expressed in terms of the value for b/a equal to 0.45 by the expression

$$\left[\frac{\lambda_c}{a} \right]_{b/a} = \left[\frac{\lambda_c}{a} \right]_{0.45} + \left[\frac{b}{a} - 0.45 \right] F \quad (11)$$

where F is the correction factor and is a function of b/a .

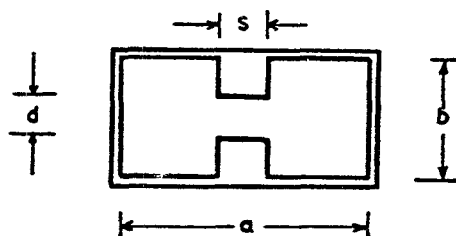
Computed values of F against b/a are plotted in Figs. 5 to 13 for the following ridge parameters:

$$s/a = 0.1 (0.1) 0.9$$

$$d/b = 0.1 (0.1) 0.9.$$

TABLE II
COMPUTED VALUES OF λ_c/a FOR $b/a=0.45$ - DOUBLE RIDGE

s/a	0.05	0.10	0.15	0.20	0.25	0.30	0.35	0.40	0.45	0.50	0.55	0.60	0.65	0.70	0.75	0.80	0.85	0.90	0.95
0.05	4.414	3.604	3.224	2.982	2.806	2.669	2.558	2.465	2.386	2.318	2.259	2.208	2.163	2.125	2.092	2.064	2.041	2.023	2.009
0.10	5.212	4.070	3.551	3.231	3.005	2.832	2.693	2.579	2.482	2.399	2.327	2.265	2.210	2.163	2.122	2.087	2.057	2.033	2.014
0.15	5.825	4.439	3.816	3.436	3.170	2.968	2.807	2.675	2.564	2.469	2.386	2.315	2.252	2.197	2.149	2.108	2.073	2.043	2.019
0.20	6.304	4.732	4.029	3.602	3.304	3.080	2.901	2.755	2.632	2.527	2.436	2.357	2.288	2.227	2.173	2.126	2.086	2.052	2.023
0.25	6.678	4.963	4.197	3.733	3.411	3.168	2.977	2.820	2.688	2.575	2.477	2.392	2.317	2.251	2.193	2.142	2.098	2.059	2.027
0.30	6.965	5.139	4.325	3.833	3.492	3.236	3.034	2.869	2.730	2.611	2.509	2.419	2.340	2.271	2.209	2.155	2.107	2.066	2.030
0.35	7.174	5.266	4.416	3.904	3.549	3.283	3.074	2.903	2.759	2.637	2.531	2.438	2.357	2.285	2.221	2.164	2.114	2.070	2.032
0.40	7.313	5.348	4.473	3.947	3.583	3.311	3.097	2.922	2.776	2.652	2.544	2.450	2.367	2.293	2.228	2.170	2.119	2.074	2.034
0.45	7.385	5.386	4.497	3.963	3.595	3.320	3.104	2.928	2.781	2.656	2.547	2.453	2.370	2.296	2.231	2.173	2.121	2.075	2.035
0.50	7.392	5.381	4.489	3.953	3.584	3.310	3.094	2.919	2.773	2.649	2.542	2.448	2.366	2.294	2.229	2.172	2.121	2.075	2.035
0.55	7.334	5.334	4.447	3.916	3.551	3.280	3.068	2.896	2.753	2.631	2.527	2.436	2.356	2.286	2.223	2.167	2.118	2.074	2.035
0.60	7.211	5.243	4.373	3.852	3.496	3.232	3.025	2.859	2.720	2.603	2.503	2.416	2.339	2.272	2.212	2.160	2.112	2.070	2.031
0.65	7.018	5.106	4.263	3.760	3.417	3.163	2.965	2.806	2.675	2.564	2.469	2.388	2.316	2.253	2.198	2.148	2.105	2.066	2.031
0.70	6.751	4.921	4.116	3.638	3.312	3.073	2.888	2.739	2.617	2.514	2.427	2.352	2.286	2.229	2.179	2.134	2.095	2.059	2.028
0.75	6.400	4.680	3.927	3.482	3.181	2.961	2.791	2.656	2.546	2.453	2.375	2.308	2.251	2.200	2.156	2.117	2.062	2.052	2.025
0.80	5.951	4.377	3.693	3.291	3.021	2.825	2.676	2.557	2.461	2.382	2.315	2.258	2.209	2.167	2.130	2.097	2.048	2.043	2.020
0.85	5.381	3.998	3.403	3.058	2.829	2.664	2.539	2.442	2.364	2.300	2.246	2.201	2.162	2.129	2.100	2.075	2.053	2.033	2.016
0.90	4.643	3.521	3.046	2.775	2.599	2.474	2.381	2.310	2.254	2.208	2.170	2.138	2.111	2.088	2.069	2.051	2.036	2.023	2.011
0.95	3.653	2.899	2.595	2.429	2.324	2.253	2.201	2.162	2.132	2.107	2.087	2.071	2.057	2.045	2.035	2.026	2.019	2.012	2.006



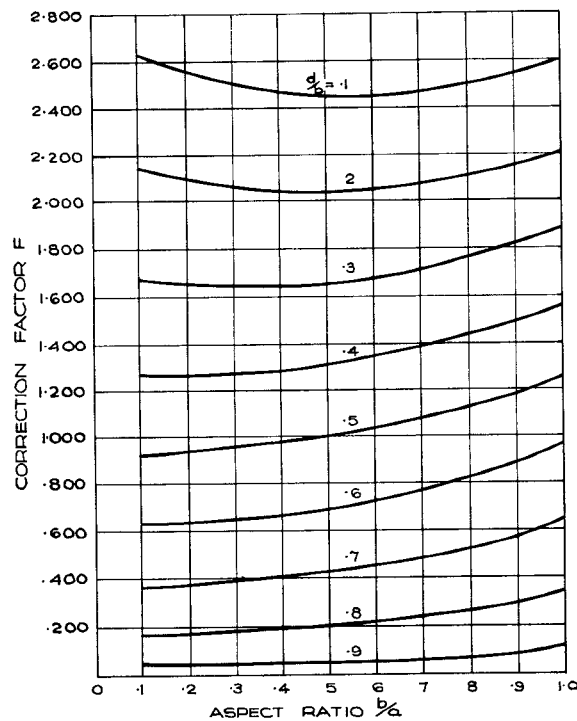


Fig. 5. Curves of correction factor F against b/a at constant ridge width $s/a = 0.1$.

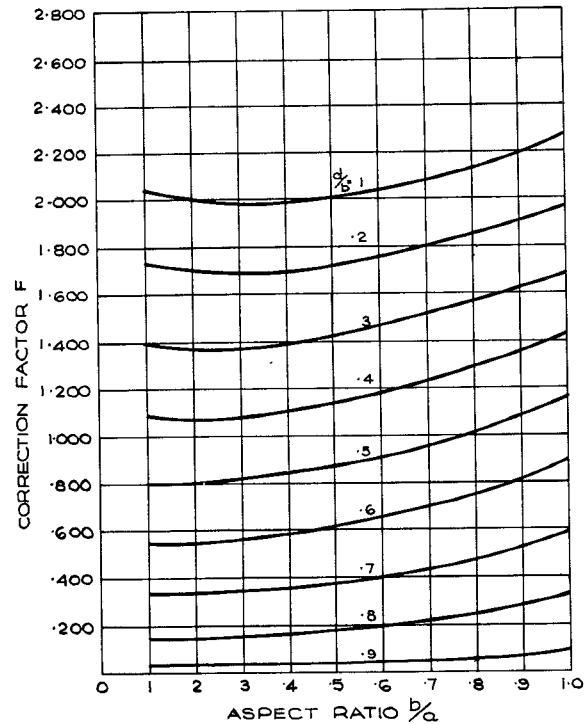


Fig. 6. Curves of correction factor F against b/a at constant ridge width $s/a = 0.2$.

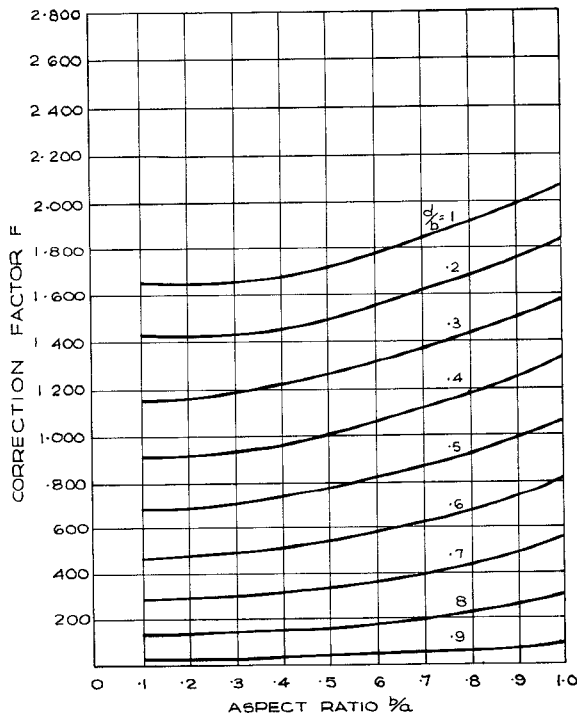


Fig. 7. Curves of correction factor F against b/a at constant ridge width $s/a = 0.3$.

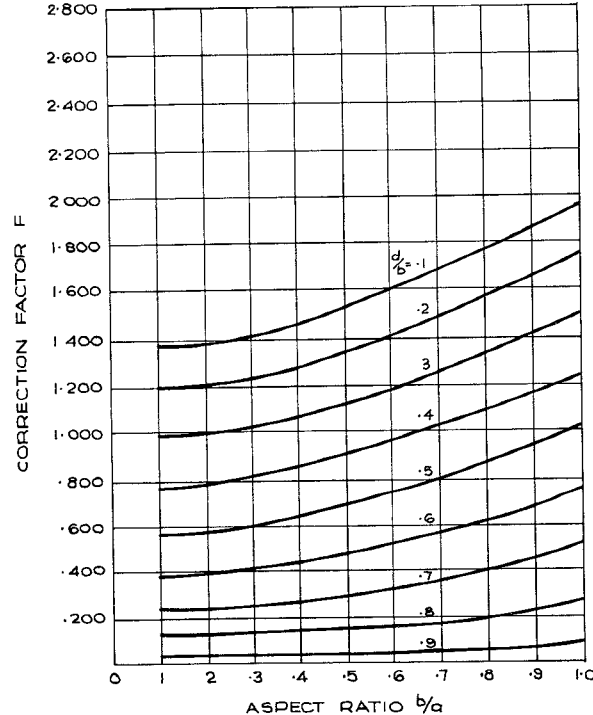


Fig. 8. Curves of correction factor F against b/a at constant ridge width $s/a = 0.4$.

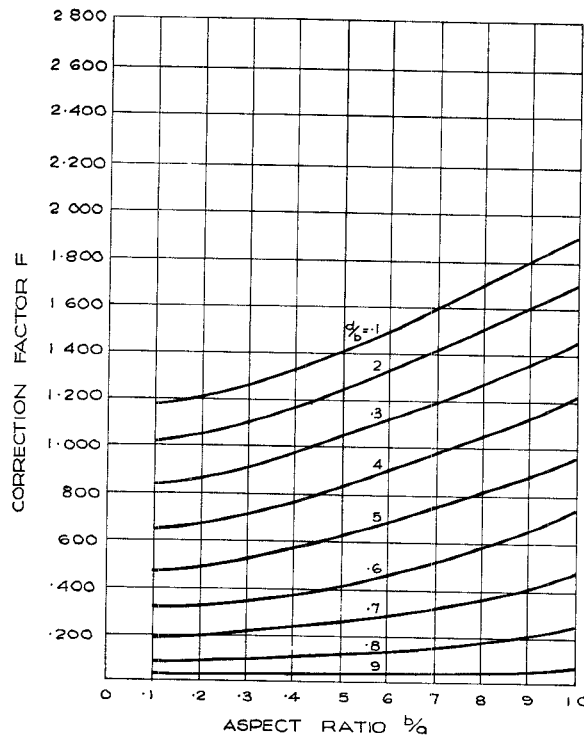


Fig. 9. Curves of correction factor F against b/a at constant ridge width $s/a = 0.5$.

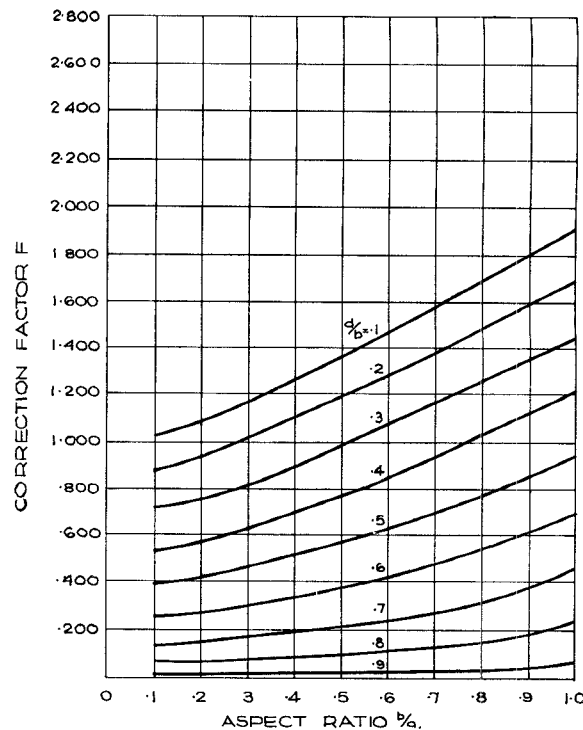


Fig. 10. Curves of correction factor F against b/a at constant ridge width $s/a = 0.6$.

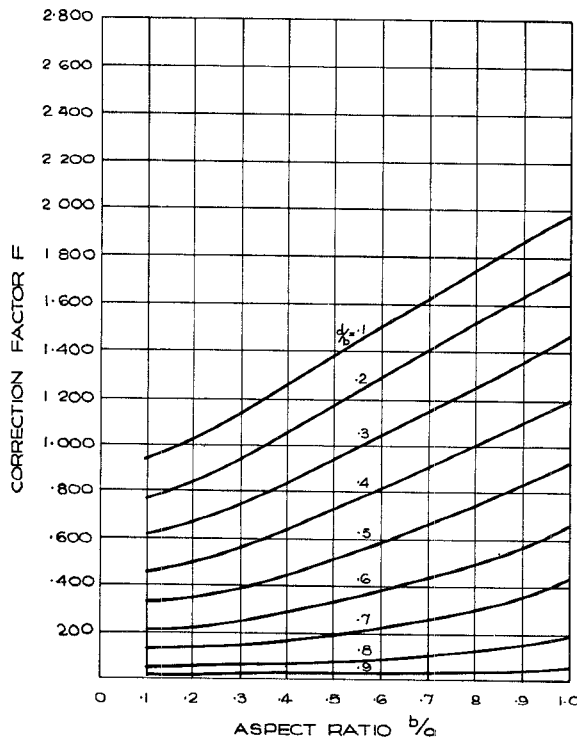


Fig. 11. Curves of correction factor F against b/a at constant ridge width $s/a = 0.7$.

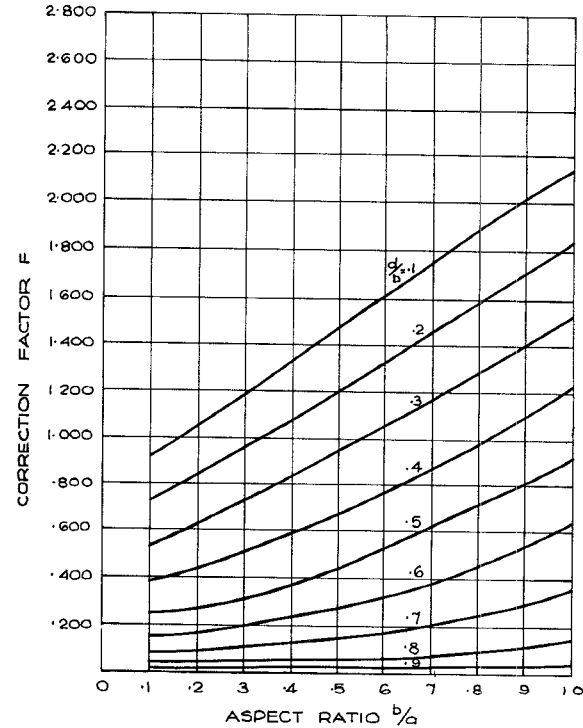


Fig. 12. Curves of correction factor F against b/a at constant ridge width $s/a = 0.8$.

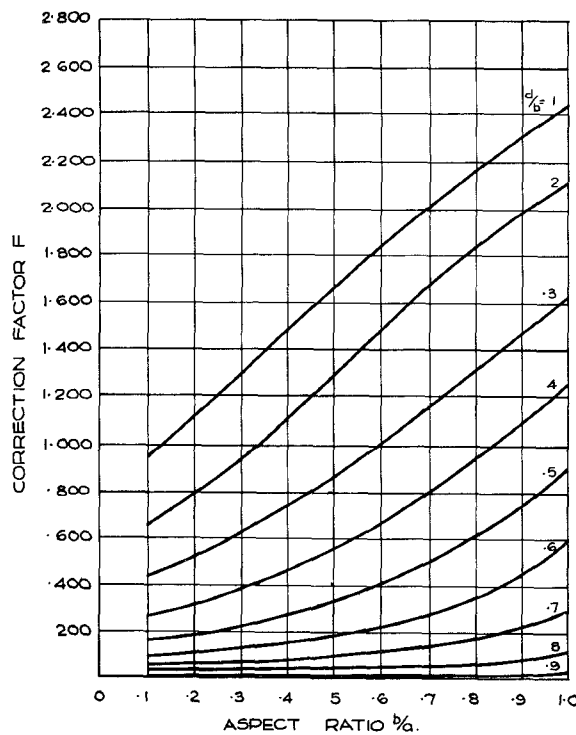


Fig. 13. Curves of correction factor F against b/a at constant ridge width $s/a = 0.9$.

VII. CONCLUSION

The cutoff wavelengths of single- or double-ridged rectangular waveguide of any aspect ratio have been computed allowing for the discontinuity susceptance of the ridge and the proximity of the ridge to the side wall of the waveguide.

The first-order correction curves given by Hopfer have been replaced by accurate correction curves which show quite definitely that the correction, or F factor, is itself a function of the b/a ratio.

An analysis of the accuracy of the design tables and graphs for the worst configurations of ridge and waveguide has shown that the computations may be in error by a few percent because of proximity effects. For design purposes, where the geometry is not likely to be critical, the tables and graphs may be used with confidence.

APPENDIX

PROXIMITY EFFECTS AND ERROR ANALYSIS

The effect of each type of proximity mentioned previously may be calculated from a relationship between the error $\Delta(\lambda_c/a)/\lambda_c/a$ in normalized cutoff wavelength and the error $\Delta C/C$ in the discontinuity capacity.

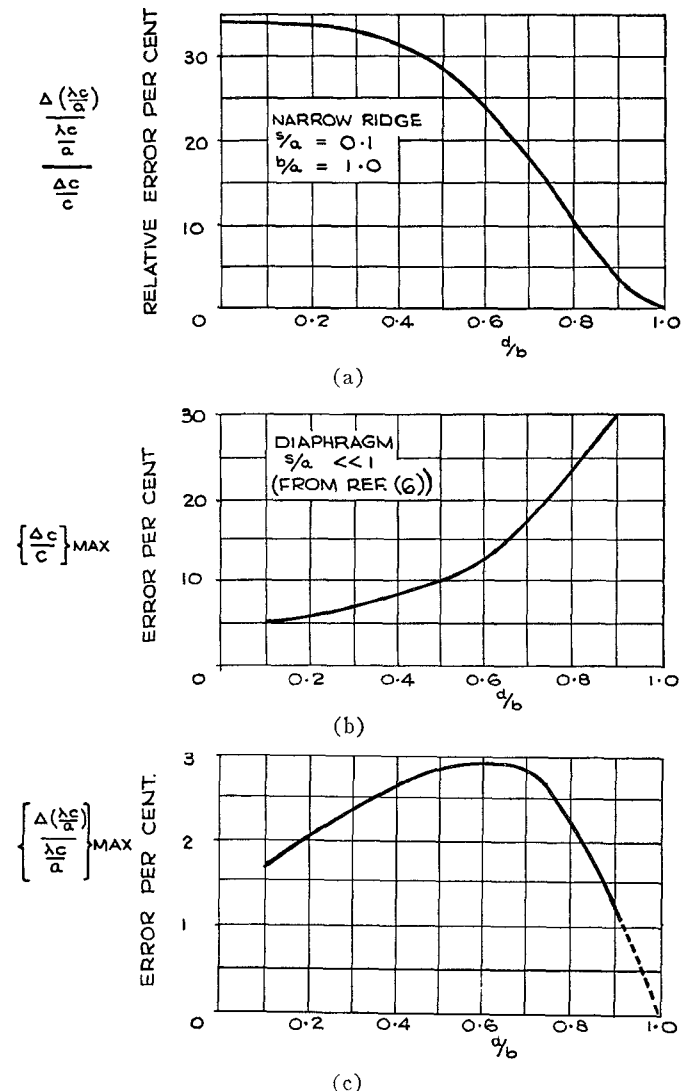


Fig. 14. Proximity effect for narrow ridges.

Starting with the cutoff condition

$$BZ_2 = \cot \phi_2 - b/d \tan \phi_1$$

where

$$\phi_1 = \pi s/\lambda_c$$

$$\phi_2 = \pi \frac{(a - s)}{\lambda_c}$$

$$B = \frac{2\pi v}{\lambda_c} \cdot C$$

$$Z_2 = \eta b$$

it may be shown by differentiating the expression with respect to λ_c and rearranging that

$$\frac{\Delta(\lambda_c/a)}{\lambda_c/a} = \frac{\cot \phi_2 - (b/d) \tan \phi_1}{\cot \phi_2 - b/d \tan \phi_1 + \frac{[\pi(1 - s/a) \cosec^2 \phi_2 + b/d \pi s/a \sec^2 \phi_1]}{\lambda_c/a}} \cdot \frac{\Delta C}{C} \quad (12)$$

This is the required relationship which is a function of the geometry (a , b , s , and d) of the ridged waveguide cross section.

Consider the first type of proximity effect where the ridge is very narrow and maximum interaction occurs between the fringing field discontinuities across the top of the ridge. The worst case given by the design graphs is that when $s/a = 0.1$ and $b/a = 1.0$. Figure 14(a) shows a plot of $\Delta(\lambda_c/a)/\lambda_c/a$ against d/b , the values being computed from (12) using the tabulated values of λ_c/a .

The maximum error in the discontinuity capacity may be obtained from Macfarlane's paper [6]. Macfarlane compared the capacity calculated for a step between infinite parallel plate lines with half of that calculated for a diaphragm (i.e., $s/a \ll 1$) of the same d/b ratio. A plot of the error $\Delta C/C$ against d/b for the above case is shown in Fig. 14(b).

The error $\Delta(\lambda_c/a)\lambda_c/a$ as a function of d/b is obtained from the corresponding values in Fig. 14(a) and Fig. 14(b); the results are plotted in Fig. 14(c). It can be seen that for the worst case of a thin diaphragm the error introduced into λ_c/a is between one and three percent.

For the second type of proximity effect where the ridge is close to the side wall of the waveguide, it is convenient to consider the analysis of a 90° bend in parallel plate line as shown in Fig. 15. Chen [7] has shown that the corner capacity C_c of a unit cube corner is given by

$$\frac{C_c}{\epsilon} = 0.558$$

where ϵ = the permittivity of the medium of the corner.

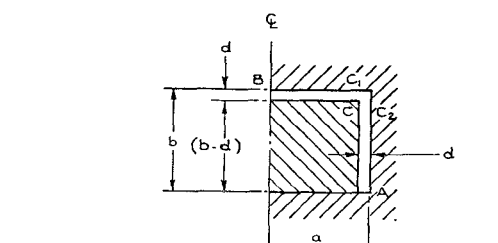
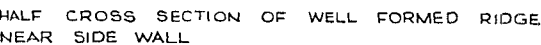
Green [8], in an unpublished paper, has determined the inductance L of the pi network representing the corner, and has shown that for a unit corner the value is μ the permeability of the medium.

The accuracy of the values for the capacity and inductance of the pi network are conditional upon:

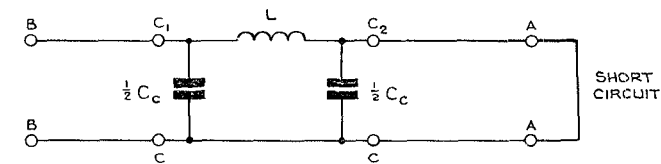
- 1) the wavelength being large compared with the dimensions of the corner, and
 - 2) the corner being well removed from external influences, e.g., a short circuit.

The above conditions are met for the worst proximity case where λ_c and $(b-d)$ are large compared with d .

The cutoff wavelength of a well-formed ridge close to the side wall of a waveguide may be determined from an analysis of the cross section shown in Fig. 15. The value of λ_c is obtained by satisfying the condition that a short circuit at A transforms to an open circuit at B . A transcendental equation in λ_c is obtained, and it is known that an approximate solution is given by the tabulated data using the coth proximity expression. For convenience, the value of λ_c/a for the condition $b/a = 0.45$, $s/a = 0.9$, and $d/b = 1/9$ was determined and compared with the value obtained from Table I. The resultant error $\Delta(\lambda_c/a)/(\lambda_c/a)$ was three percent.



EQUIVALENT CIRCUIT TO HALF SECTION



FOR A UNIT CORNER CUBE
 $C_c = .558 \epsilon$
 $L = \mu$

Fig. 15. Analysis of a well-formed ridge near the side wall of waveguide.

The error $[\Delta(\lambda_c/a)/(\lambda_c/a)]/(\Delta C/C)$ obtained from (12) under the aforementioned conditions is 10 percent, i.e., the error $\Delta C/C$ some 30 percent. It is interesting to note that the large error in C for the side wall proximity contributes only a small error in λ_c .

ACKNOWLEDGMENT

The author wishes to thank the Chief Scientist, Department of Supply, Australia for permission to publish this paper externally. The helpful discussions with H. E. Green concerning the error analysis of proximity effects have been much appreciated.

REFERENCES

- [1] N. Marcuvitz, *Waveguide Handbook*. M.I.T. RAD Lab. Series, New York: McGraw-Hill, 1951, vol. 10, pp. 399-402.
 - [2] S. B. Cohn, "Properties of ridge wave guide," *Proc. IRE*, vol. 35, pp. 783-788, August 1947.
 - [3] S. Hopfer, "The design of ridged waveguides," *IRE Trans. on Microwave Theory and Techniques*, vol. MTT-3, pp. 20-29, October 1955.
 - [4] *Op. cit.* [1], pp. 307-308.
 - [5] J. R. Whinnery and H. W. Jamieson, "Equivalent circuits for discontinuities in transmission lines," *Proc. IRE*, vol. 32, pp. 98-114, February 1944.
 - [6] G. G. Macfarlane, "Quasi-stationary field theory and its applications to diaphragms and junctions in transmission lines and waveguides," *J. Brit. IEEE*, vol. 93, pt. 3A, pp. 703-719, March-May 1946.
 - [7] T. S. Chen, "Determination of the capacitance, inductance, and characteristic impedance of rectangular lines," *IRE Trans. on Microwave Theory and Techniques*, vol. MTT-8, pp. 510-520, September 1960.
 - [8] H. E. Green, "The equivalent network of a bend in parallel plate line with applications to TEM mode transmission lines and waveguides," *WRE Tech. Note*, published March 1966¹.

¹ Green has determined the inductance of the π network representing the corner from a numerical analysis. However, he wishes to point out that the solution may be obtained from Marcuvitz's analysis of the E-plane bend in rectangular waveguide (see pp. 312-318 of Marcuvitz [1]).